

# Single qubit gates with a charged quantum dot using minimal resources

François Dubin\* and Gavin Brennen†

\*Institute for Experimental Physics, University of Innsbruck, Technikerstr. 25, A-6020 Innsbruck, Austria

†Institute for Quantum Optics and Quantum Information of the Austrian Academy of Sciences, 6020 Innsbruck, Austria

(Dated: November 20, 2018)

We investigate coherent control of a single electron trapped in a semiconductor quantum dot. Control is enabled with a strong laser field detuned with respect to the electron light-hole optical transitions. For a realistic experimental situation, i.e. with a weak magnetic field applied along the growth direction, high fidelity arbitrary rotations of the electron spin are possible using a single laser spatial mode. This makes viable quantum gates with electron spins in systems with restricted optical resources.

PACS numbers: 78.67.Hc, 03.67.Lx

## I. INTRODUCTION

A large research effort is presently devoted to the manipulation of an increasing number of quantum systems in order to use them as a possible support for quantum computation. In atomic physics, on the one side single trapped ions have lead to major steps toward large scale quantum hardware. The almost perfect control of trapped ions motional and electronic long lived states has enabled high fidelity single qubit operations<sup>1</sup>, very efficient two qubit gates<sup>2</sup> and recently the realization of the first quantum-bite<sup>3</sup>. On the other side, cold atomic ensembles are also very attractive and have emerged as an alternative light-matter interface. Quantum state transfer from an atomic cloud onto a photonic qubit has been demonstrated<sup>4</sup> as well as the entanglement of two remote atomic ensembles<sup>5</sup>.

In solid state physics, charged semiconductor quantum dots are also promising candidates to implement quantum computing protocols. A single trapped electron in a quantum dot has long lived spin states<sup>6</sup> which in principle allow for long information storage times. Very recently, the spin state of a single electron trapped in a self assembled quantum dot has been prepared with a fidelity close to unity<sup>7</sup>. This initialization, prerequisite to any spin manipulation, is a major advance which can be seen as a laser-cooling mechanism implemented in a solid-state environment. In the experiments of Atatüre and coworkers, a weak magnetic field ( $\approx 100$  mT) was applied along the quantum dot growth direction (Faraday configuration) such that the electron spin state becomes less sensitive to surrounding fluctuations. In many other works, single charged quantum dots are also studied when a strong magnetic field ( $\approx 5$ -10 T) is applied perpendicular to the growth axis<sup>8</sup> (Voigt configuration). The latter removes the degeneracy of the two spin projections along the field which are then the basis for subsequent manipulations. In the Voigt configuration electron spin coherences have been measured<sup>9</sup> while theoretical proposals have shown how optical control can be achieved<sup>10,11</sup>.

A trapped electron spin can be rotated in different ways, in general due to subtle fermion exchanges

which can take place with virtual excitons coupled to unabsorbed photons<sup>12</sup>. In quantum dots, when a strong magnetic field is applied in the Voigt configuration, Raman transitions have been proposed to perform arbitrary single qubit operations<sup>10,11</sup>. Using two crossed polarized and detuned laser pulses, the electron spin states can be virtually coupled to "trion" states<sup>13</sup>. The trapped electron spin can therefore be well manipulated, with a close to unity fidelity for typical operation times of 50 ps. A procedure to perform general spin rotations via Stimulated Raman Adiabatic Passage (STIRAP) was also proposed<sup>14</sup>, with a required auxiliary ground state, to perform single qubit operations and quantum gates in coupled quantum dots.

In this work, we show that the spin state of a single charged quantum dot can also be completely controlled with a single laser frequency, with or without a weak magnetic field applied in the Faraday configuration. The latter situation corresponds to experiments which have up to now provided remarkable results, furthermore, removing the degeneracy protects the qubit from spin flipping errors. Using a single laser beam, of prepared elliptical polarization and tilted with respect to the quantum dot growth direction, a coherent coupling between the two electron spin states is created. Arbitrary rotations can thereby be obtained in few tens of picoseconds, with high fidelities for realistic experimental parameters. We derive the photon induced entanglement of the electron spin states through an effective Hamiltonian describing the virtual transitions towards trion states. The mechanism is highlighted by the recently developed Shiva diagrams for interacting composite bosons<sup>12</sup>.

Our proposal is based on the semiconductor light-hole excitations. In a GaAs quantum well, the latter have allowed the experimental demonstration of an induced electron spin coherence, in a waveguide geometry i.e. with an excitation laser propagating in the plane of the quantum well<sup>15</sup>. In the experiments of Sarkar et al., a light-hole relaxation time of about 40 ps is deduced. This value at first seems to prohibit the use of light-holes for any electron spin manipulation. The same order of magnitude is indeed expected for self-

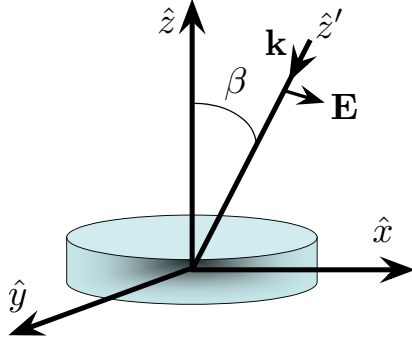


FIG. 1: Sketch of the considered experimental configuration. The laser beam propagates in the  $(Oxz)$  plane of a self-assembled quantum dot, at an angle  $\beta$  with respect to the  $\hat{z}$  axis. The laser polarization  $\mathbf{E}$  is in general elliptical and has projection along  $\hat{x}, \hat{y}, \hat{z}$ .

assembled quantum dots (to our best knowledge, in quantum dots no experimental values for the light-hole lifetime have been reported). However, we will demonstrate in the following that high-fidelity qubit gates can be achieved using light-holes. In the worst case scenario for which light-holes would have a lifetime of 50 ps in a quantum dot, we show that arbitrary rotations of the electron spin already have at least 97% fidelities with a gate time of few tens of picoseconds.

In strained quantum dots, light-hole levels can become the lowest energy hole states<sup>17</sup>. This suppresses most relaxation channels and yields long lived light-holes. Assuming such a quantum dot, Calarco and co-workers<sup>18</sup> have proposed to use Raman transitions between electron and light-hole states to perform single qubit rotations and two qubit gates. With two orthogonal laser fields, of linear and circular polarizations, the electron spin states can indeed be coherently coupled. In this work, we show that the resulting complex two orthogonal axes geometry is in fact not required, a single laser beam of suitable elliptical polarization and propagation direction is sufficient. Using a single beam provides more optical access for scattered light which improves photon detection efficiency.

## II. SETUP

As shown in Figure 1, we consider an excitation laser which propagates in the  $(Oxz)$  plane of a self-assembled quantum dot at an angle  $\beta$  relative to the  $\hat{z}$  axis. In the most general situation, the laser field polarization has non vanishing projections along all directions,  $\hat{x}, \hat{y}$ , and  $\hat{z}$ . The first two are used to couple light-hole levels to the two electronic levels via  $\sigma^+$  and  $\sigma^-$  optical transitions. The last projection also couples the light-hole levels to the electronic ones but via so called

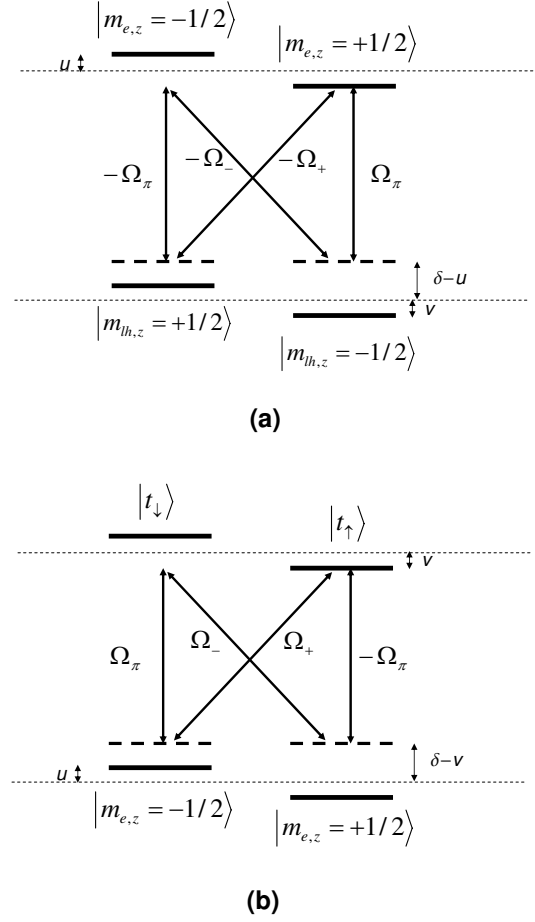


FIG. 2: (a) Optically allowed transitions between the electron and the light-hole levels. The Rabi frequencies are defined in the text. (b) Optical transitions when considering that the electronic states are coupled to trions. Note that in this second representation the different coupling strengths have different signs.

$\pi$  transitions maintaining the projection of the angular momentum along  $(Oz)$  (see Figure 2.a). Consequently, a coherent coupling between the trapped electron states, with up and down spin projections along  $(Oz)$ , can be induced. Moreover, since semiconductors have a refractive index of the order of 3.5, the angle can be  $|\beta| \lesssim 20^\circ$ .

The carrier exchange between the trapped real electron and the virtual light-hole-electron pair, coupled to unabsorbed  $\pi$ ,  $\sigma_+$  or  $\sigma_-$  photons, allows to switch the trapped electron spin projection along  $(Oz)$  (see Figure 3). This switch imposes the transformation of a  $\pi$  photon into a  $\sigma_+$  or a  $\sigma_-$  one, or vice-versa, in order to conserve the total momentum of the system. Note that, in these processes, the intermediate states are made of one real and one virtual electron with opposite spins, along with one virtual light-hole. The optical spin manipulation we propose then implies the formation of a

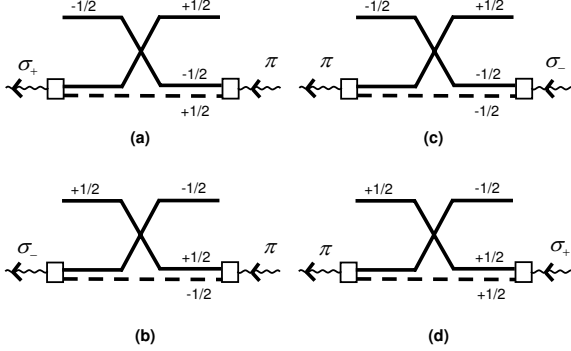


FIG. 3: Diagrammatic representation of the physical processes involved in the electron spin-flip. The wavy line represents pump photons, the full and dashed lines correspond to the electron and light-hole respectively. (a) Exchange interaction leading to the trapped electron spin-flip and the transformation of a  $\pi$  photon into a  $\sigma^+$  one. (b)  $\sigma^-$  photons can also be obtained from  $\pi$  ones while flipping the electron spin. (c) and (d): Electron spin-flip obtained from the transformation of  $\sigma$  photons into  $\pi$  ones.

semi virtual trion, in the same way as in Ref<sup>11</sup>.

### III. FORMALISM FOR THE SPIN FLIP OF A TRAPPED ELECTRON

#### A. Photon and dot Hamiltonians

We consider unabsorbed photons with a detuning  $\delta$  with respect to the electron-light-hole transition, i.e. with a frequency

$$\omega = E_e + E_{lh} + \delta, \quad (1)$$

$E_e$  and  $E_{lh}$  being the electron and light-hole energies without applied magnetic field respectively. In self assembled quantum dots, the energy splitting between the heavy and the light-holes levels is typically of the order of tens of meV, while the energy splitting between the confined electronic levels can be made much larger for small dot structures<sup>19</sup>. Consequently, in the following we only consider couplings between the light-holes and the first confined electronic state, the laser photons being assumed far detuned with other electronic transitions.

In a quantum dot small compared to the exciton Bohr radius, the Coulomb interaction is rather unimportant, the carrier energy being controlled by localization. In addition, as already shown on various examples<sup>20</sup>, the optical non linearities are driven by pure carrier exchanges, due to a bare dimensionality argument, so that

Coulomb interaction between carriers is going to play a minor role in the problem investigated here. This is why Coulomb interactions can be neglected in the dot Hamiltonian reducing to

$$H_d = \sum_{s=\pm 1/2} \hbar \omega_s a_s^\dagger a_s + \sum_{s=\pm 1/2} \hbar \omega_{\frac{3}{2},s} b_{\frac{3}{2},s}^\dagger b_{\frac{3}{2},s}. \quad (2)$$

$a$  ( $a^\dagger$ ) and  $b$  ( $b^\dagger$ ) being fermionic operators for the destruction (creation) of a trapped electron or hole respectively.

#### B. Dot-photon interaction

The semiconductor-laser-photons interaction is in general written as  $W = V + V^\dagger$ , where  $V^\dagger = V_+^\dagger + V_-^\dagger + V_0^\dagger$  with

$$\begin{aligned} V_+^\dagger &= \lambda_+ \left( a_{-\frac{1}{2}}^\dagger b_{\frac{3}{2},\frac{3}{2}}^\dagger - \sqrt{\frac{1}{3}} a_{\frac{1}{2}}^\dagger b_{\frac{3}{2},\frac{1}{2}}^\dagger - \sqrt{\frac{2}{3}} a_{\frac{1}{2}}^\dagger b_{\frac{1}{2},\frac{1}{2}}^\dagger \right) \\ V_-^\dagger &= -\lambda_- \left( a_{\frac{1}{2}}^\dagger b_{\frac{3}{2},-\frac{3}{2}}^\dagger + \sqrt{\frac{1}{3}} a_{-\frac{1}{2}}^\dagger b_{\frac{3}{2},-\frac{1}{2}}^\dagger \right. \\ &\quad \left. - \sqrt{\frac{2}{3}} a_{-\frac{1}{2}}^\dagger b_{\frac{1}{2},-\frac{1}{2}}^\dagger \right) \\ V_0^\dagger &= \sqrt{\frac{2}{3}} \lambda_0 \left( a_{\frac{1}{2}}^\dagger b_{\frac{3}{2},-\frac{1}{2}}^\dagger - a_{-\frac{1}{2}}^\dagger b_{\frac{3}{2},\frac{1}{2}}^\dagger + a_{\frac{1}{2}}^\dagger b_{\frac{1}{2},-\frac{1}{2}}^\dagger \right. \\ &\quad \left. + a_{-\frac{1}{2}}^\dagger b_{\frac{1}{2},\frac{1}{2}}^\dagger \right) \end{aligned} \quad (3)$$

The photon field is treated classically, with the definition  $\lambda_{0,\pm} = ePA_{0,\pm}/\omega mc^{21}$ , where  $\mathbf{A}$  is the field vector potential,  $m$  is the electron mass, and  $P$  is the canonical momentum whose vector components are identical. Restricting to the light-hole levels, we only consider couplings employing the  $b_{\frac{3}{2},\pm\frac{1}{2}}$  operators.

The coupling  $W$  does not conserve the number of carriers, the changes it induces to the degenerate zero,  $|vac\rangle$ , and one electron states  $|\pm 1/2\rangle$  only appear at second order in this coupling. In order to derive the dynamics in the  $m_s = \pm 1/2$  trapped electron states in the presence of pump photons, we express an effective Hamiltonian,  $H_{\text{eff}}$ , to obtain proper equations of motion. In this approach, several constraints are imposed. Apart from hermiticity, most importantly,  $H_{\text{eff}}$  must have the same eigenvalues as the original Hamiltonian,  $H = H_d + W$ , with the same degeneracy.  $H_{\text{eff}}$  is in fact obtained from an appropriate unitary transformation<sup>22</sup>, and reads at second order in the coupling  $W$

$$H_{\text{eff}} = H_d + \frac{1}{2} \sum_{k,s,s'} |s\rangle \langle s| W |k\rangle \langle k| W \left( \frac{1}{E_s + \omega - E_k} + \frac{1}{E_{s'} + \omega - E_k} \right) |s'\rangle \langle s'| \quad (4)$$

where the states  $|k\rangle$  correspond to any intermediate states and  $|s\rangle, |s'\rangle$  are initial and final ground states respectively.

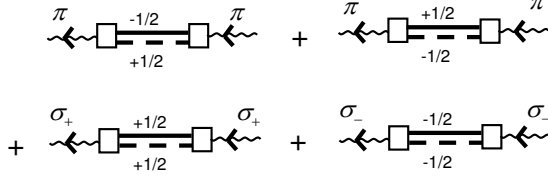


FIG. 4: Different contributions to the energy change of the zero electron state,  $|vac\rangle$ .

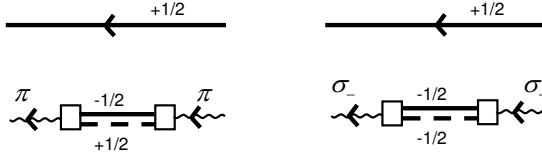


FIG. 5: Diagonal processes for a trapped electron with  $m_s = +1/2$  spin projection along  $\hat{z}$ .

### C. Couplings of the zero electron states

The dot-photon interaction induces an energy shift of the zero-electron state,  $|vac\rangle$ . It is given by the matrix elements of  $H_{\text{eff}}$  in this degenerate subspace. From eqs. (1-4) it is easy to show that this operator is diagonal, with

$$\begin{aligned} \langle vac | H_{\text{eff}} | vac \rangle = & \frac{2}{3} \frac{|\lambda_0|^2}{\delta + (u+v)} + \frac{2}{3} \frac{|\lambda_0|^2}{\delta - (u+v)} \\ & + \frac{1}{3} \frac{|\lambda_+|^2}{\delta + (u-v)} + \frac{1}{3} \frac{|\lambda_-|^2}{\delta - (u-v)} \end{aligned} \quad (5)$$

$u$  and  $v$  being the electron and light-hole energy shifts induced by the applied magnetic field. Note that these are very small compared to  $\delta$  for our parameter regime of interest. We remark that two channels exist for the coupling of  $\pi$  photons with the dot electron-light-hole states, while there is only one channel for the circularly polarized photons. The different terms of eq.(5) are shown in Figure 4.

### D. Couplings of the one electron states

The modifications induced by the trapped electron-photon interaction contain two types of processes.

(i) In direct processes, the electron which recombines is the one of the virtual electron-hole pair coupled to the excitation photon. Due to Pauli exclusion, the electron of the virtual pair must however have a spin different from the one already present in the quantum dot. For an  $m_s = +1/2$  electron, we only have the two processes shown in Figure 5. The energy change induced for these diagonal processes is

$$\langle \frac{1}{2} | H_{\text{eff}} | \frac{1}{2} \rangle = -u + \frac{2}{3} \frac{|\lambda_0|^2}{\delta - (u-v)} + \frac{1}{3} \frac{|\lambda_-|^2}{\delta - (u+v)} \quad (6)$$

(ii) Exchange processes are also possible between the trapped electron and the virtual electron-light-hole pair coupled to photons. Again, due to the Pauli exclusion principle, the electron spin of this virtual pair must be different from the trapped one. An electron exchange between a virtual pair coupled to a  $\pi$  photon and a  $m_s = 1/2$  electron leads to the diagram of Figure 3.a, while an electron exchange with a  $m_s = -1/2$  electron leads to the diagram of Figure 3.b. In this exchange, the spin of the trapped electron flips while a  $\pi$  photon is transformed into a circularly polarized photon. The reverse transformations being also allowed (see Figures 3.c and 3.d), these processes lead to the two non diagonal matrix elements

$$\begin{aligned} \langle \frac{1}{2} | H_{\text{eff}} | -\frac{1}{2} \rangle = & -\left( \frac{\sqrt{2}}{3} \lambda_0 \lambda_+^* \frac{\delta+v}{(\delta+v)^2 - u^2} \right. \\ & \left. - \frac{\sqrt{2}}{3} \lambda_0^* \lambda_- \frac{\delta-v}{(\delta-v)^2 - u^2} \right) \\ = & \langle -\frac{1}{2} | H_{\text{eff}} | \frac{1}{2} \rangle^* \end{aligned} \quad (7)$$

the minus sign being due to the single carrier exchange involved in these interactions. Therefore, we obtain in the computational basis  $\{ |-\frac{1}{2}\rangle, |\frac{1}{2}\rangle \}$

$$H_{\text{eff}} = \begin{bmatrix} u + \frac{|\Omega_\pi|^2}{\delta-v+u} + \frac{|\Omega_+|^2}{\delta+u+v} & \frac{\Omega_\pi^* \Omega_- (\delta-v)}{(\delta-v)^2 - u^2} - \frac{\Omega_\pi \Omega_+^* (\delta+v)}{(\delta+v)^2 - u^2} \\ \frac{\Omega_\pi \Omega_-^* (\delta-v)}{(\delta-v)^2 - u^2} - \frac{\Omega_\pi^* \Omega_+ (\delta+v)}{(\delta+v)^2 - u^2} & -u + \frac{|\Omega_\pi|^2}{\delta-u+v} + \frac{|\Omega_-|^2}{\delta-u-v} \end{bmatrix} \quad (8)$$

with  $\Omega_\pi = \sqrt{2/3} \lambda_0$ ,  $\Omega_+ = \sqrt{1/3} \lambda_+$  and  $\Omega_- = \sqrt{1/3} \lambda_-$ . Please note that the time dependance of these Rabi frequencies is implicitly considered.

Let us mention that in previous works<sup>10,11</sup> a density matrix approach has been followed to describe stimulated Raman transitions in quantum dots. One then

considers the four following states: the two electronic levels with spin projections in the  $\hat{z}$  direction,  $|+1/2\rangle$  and  $|-1/2\rangle$ , and the two trion levels  $|t_\uparrow\rangle$  and  $|t_\downarrow\rangle$  made of an electron pair with opposite spins and a light hole with up and down spin projection along  $\hat{z}$  respectively. The level scheme and the different optical transition strengths are depicted in Figure 2.b. Please note that to preserve proper anti-commutation relations between fermionic operators, the optical transitions have in this point of view different signs compared to the previous expressions. A model Hamiltonian can thus be built in the  $\{|1/2\rangle, |-1/2\rangle, |t_\uparrow\rangle, |t_\downarrow\rangle\}$  basis, and turning into the rotating frame, the equations of motion in the restricted  $\{|+1/2\rangle, |-1/2\rangle\}$  subspace are obtained after adiabatic elimination of the virtually populated trion levels. This procedure provides the proper effective Hamiltonian in second order perturbation theory, but let us stress that care must be taken in order to correctly account for non degeneracy of the ground states.

#### IV. BUILDING SINGLE QUBIT ROTATIONS

Consider the geometry in Fig. 1 with the  $\hat{z}$  axis defined as the axis of symmetry of the quantum dot. The addressing laser propagates with a wavevector  $\mathbf{k}$  at an angle  $\beta$  with respect to the  $\hat{z}$  axis in the  $(Oxz)$  plane. We choose an elliptical polarization of the electric field with respect to a primed coordinate frame ( $\hat{z}' \equiv \hat{k}$ ) given by  $\mathbf{E}'(\mathbf{x}, t) = E e^{i(\mathbf{k} \cdot \mathbf{x} - \omega t)} (\cos \gamma \mathbf{e}'_- + e^{i\phi} \sin \gamma \mathbf{e}'_+)$ . The field components in the spherical basis of the unprimed coordinate system of the dot are given by  $\mathbf{E}(\mathbf{x}, t) = D^{(1/2)\dagger}(\beta) \mathbf{E}'(\mathbf{x}, t)$ , where  $D^{(1/2)}$  is the reduced Wigner rotation matrix for a spin-1/2 representation of  $SU(2)$ <sup>23</sup>.

During single qubit gate operations, there will be decoherence induced by off resonant laser coupling to unstable trion states. We describe such decay processes by a phenomenological parameter  $\Gamma$ . The effect of this decay on gate performance is captured by constructing an effective non Hermitian Hamiltonian  $\tilde{H}_{\text{eff}}$  from  $H_{\text{eff}}$  by the replacement  $\delta \rightarrow \delta - i\Gamma/2$ . The dot-photon interaction can then be represented as a vector in the operator space spanned by the Pauli operators. Ignoring the component of the identity operator, we write  $\tilde{H}_{\text{eff}} = \hbar \Gamma (\vec{h}^R + i\vec{h}^I) \cdot \vec{\sigma}$ . In the limit  $u, v \ll \delta$ , the real parts of the dimensionless coupling vectors are

$$\begin{aligned} h_x^R &= \frac{\kappa_3 \kappa_4^2 \sin \beta \cos \beta (4 \cos \phi \cos \gamma \sin \gamma - 2)}{4 \kappa_3^2 + 1} \\ h_y^R &= \frac{2 \kappa_3 \kappa_4^2 \sin \beta \sin 2\gamma \sin \phi}{4 \kappa_3^2 + 1} \\ h_z^R &= \kappa_1 - \frac{\kappa_3 \kappa_4^2 \cos \beta \cos 2\gamma}{4 \kappa_3^2 + 1} \end{aligned} \quad (9)$$

The system parameters, which are assumed fixed during gate operations, are  $\kappa_1 = u/\hbar\Gamma$ ,  $\kappa_2 = v/\hbar\Gamma$ ,  $\kappa_3 = \delta/\Gamma$ ,  $\kappa_4 = \Omega/\Gamma$ . The Rabi frequency

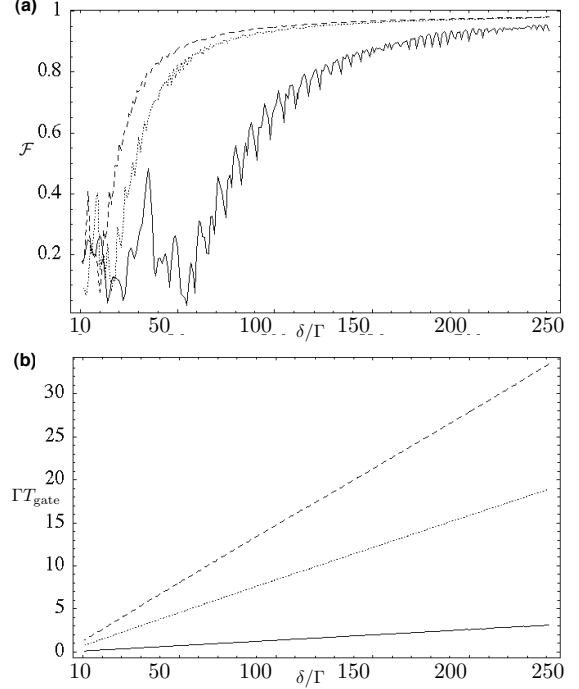


FIG. 6: Single qubit gate performance as a function of field detuning  $\delta$ . The system parameters are  $u/\hbar\Gamma = 0.1$ ,  $v/\hbar\Gamma = 0.2$ ,  $\beta = \pi/10$  and three different field strengths are plotted: solid lines correspond to  $\Omega/\Gamma = 50$ , dotted lines  $\Omega/\Gamma = 20$ , and dashed lines  $\Omega/\Gamma = 15$ . (a) Worst case fidelity for a single qubit operation. (b) Maximum gate time.

$\Omega = -\sqrt{2/3} P E e / m \omega$  and  $\Gamma$  is the parameter describing decay of the electron-light-hole pair.

Single qubit gates can be performed by using a sequence of laser pulses with varying polarization parameters  $(\gamma, \phi)$ . Because these pulses share the same wavevector  $\mathbf{k}$ , they can be obtained from the same source and used in the same geometric configuration relative to the dot. The nature of the sequence follows from the canonical decomposition of any unitary  $U \in SU(2)$ :

$$U = e^{i\vec{\xi} \cdot \vec{\sigma}} = (e^{-i\mu_3 \hat{n}_1 \cdot \vec{\sigma}}) (e^{-i\mu_2 \hat{n}_2 \cdot \vec{\sigma}}) (e^{-i\mu_1 \hat{n}_1 \cdot \vec{\sigma}}), \quad (10)$$

provided the Bloch vectors are orthogonal:  $\hat{n}_1 \cdot \hat{n}_2 = 0$ . Expanding this generalized Euler decomposition gives the following relations

$$\begin{aligned} \cos \xi &= \cos \mu_2 \cos(\mu_1 + \mu_3) \\ \hat{n}_1 \sin \xi &= -\hat{n}_1 \cos \mu_2 \sin(\mu_1 + \mu_3) - \hat{n}_2 \sin \mu_2 \cos(\mu_1 - \mu_3) \\ &\quad + \hat{n}_1 \times \hat{n}_2 \sin \mu_2 \sin(\mu_1 - \mu_3) \end{aligned}$$

These equations can be inverted and without loss of generality we can choose  $\mu_i > 0$ . Hence it is only required that for a fixed set of parameters  $\{\kappa_i\}$ , we find a pair of non zero vectors satisfying  $\vec{h}^R(\gamma_1, \phi_1) \cdot \vec{h}^R(\gamma_2, \phi_2) = 0$ .



The process fidelity can be quantified by the overlap of the target unitary  $U$  with the implemented operator. We model the implemented operator as the non unitary evolution generated by three sequential evolutions by the non-Hermitian Hamiltonian  $\tilde{H}_m$  acting on the joint electron-trion space:

$$\begin{aligned} \tilde{H}_m = & \hbar\Gamma \left[ \kappa_1 \left( \left| -\frac{1}{2} \right\rangle \left\langle -\frac{1}{2} \right| - \left| \frac{1}{2} \right\rangle \left\langle \frac{1}{2} \right| \right) \right. \\ & + (\kappa_2 - \kappa_3 - i/2) |t_\downarrow\rangle \langle t_\downarrow| - (\kappa_2 + \kappa_3 + i/2) |t_\uparrow\rangle \langle t_\uparrow| \\ & + \left( \frac{\kappa_4}{\sqrt{2}} (e^{-i\phi} \sin \gamma \cos^2 \frac{\beta}{2} + \cos \gamma \sin^2 \frac{\beta}{2}) \left| -\frac{1}{2} \right\rangle \left\langle t_\uparrow \right| \right. \\ & + \frac{\kappa_4}{\sqrt{2}} \sin \beta (e^{-i\phi} \sin \gamma - \cos \gamma) \left( \left| -\frac{1}{2} \right\rangle \left\langle t_\downarrow \right| - \left| \frac{1}{2} \right\rangle \left\langle t_\uparrow \right| \right) \\ & \left. \left. + \frac{\kappa_4}{\sqrt{2}} (\cos \gamma \cos^2 \frac{\beta}{2} + e^{-i\phi} \sin \gamma \sin^2 \frac{\beta}{2}) \left| \frac{1}{2} \right\rangle \left\langle t_\downarrow \right| \right) \right] + h.c. \end{aligned} \quad (11)$$

Hence we adopt the following measure of operator fidelity:

$$\mathcal{F} = \frac{1}{2} \left| \text{Tr} \left[ U^\dagger P_g e^{-it_3 \tilde{H}_m / \hbar} e^{-it_2 \tilde{H}_m / \hbar} e^{-it_1 \tilde{H}_m / \hbar} P_g \right] \right| \quad (12)$$

where

$$U = \exp \left[ -it_3 \vec{h}^R(\gamma_1, \phi_1) \cdot \vec{\sigma} \right] \exp \left[ -it_2 \vec{h}^R(\gamma_2, \phi_2) \cdot \vec{\sigma} \right] \times \exp \left[ -it_1 \vec{h}^R(\gamma_1, \phi_1) \cdot \vec{\sigma} \right].$$

and  $P_g$  is the projector onto the computational basis. In terms of the parameterization for  $U$ ,  $t_1 = \mu_1 / \Gamma |\vec{h}^R(\gamma_1, \phi_1)|$ ,  $t_2 = \mu_2 / \Gamma |\vec{h}^R(\gamma_2, \phi_2)|$ , and  $t_3 = \mu_3 / \Gamma |\vec{h}^R(\gamma_1, \phi_1)|$ . The worst case fidelity for building a generic gate is estimated by assuming  $\mu_i = \pi \forall i$  (see Fig. 6).

In order to construct arbitrary single qubit gates using Eq. 10 we can set  $\phi_1 = \pi, \phi_2 = 0$  such that  $h_y(\gamma_1, \phi_1) = h_y(\gamma_2, \phi_2) = 0$ . Furthermore, it suffices to choose  $\gamma_1 = \gamma_2 + \pi/2 \equiv \gamma$ . For a given set  $\{\kappa_i\}$  it is then possible to solve for  $\gamma$  such that  $\vec{h}^R(\gamma, \pi) \cdot \vec{h}^R(\gamma - \pi/2, 0) = 0$ . For example consider a setup with  $\kappa_1 = 0.1, \kappa_2 = 0.2, \kappa_3 = 250, \kappa_4 = 20, \beta = \pi/10$ . The following sequence simulates the Hadamard gate  $H$  (up to a global phase):

$$\begin{aligned} H = & \frac{1}{\sqrt{2}} \begin{pmatrix} 1 & 1 \\ 1 & -1 \end{pmatrix} \\ = & ie^{-i\Gamma t_3 \vec{h}^R(\gamma, \pi) \cdot \vec{\sigma}} e^{-i\Gamma t_2 \vec{h}^R(\gamma - \pi/2, 0) \cdot \vec{\sigma}} e^{-i\Gamma t_1 \vec{h}^R(\gamma, \pi) \cdot \vec{\sigma}}, \end{aligned} \quad (13)$$

in the basis  $\{|-1/2\rangle, |1/2\rangle\}$ . Here the field setting is  $\gamma = 0.4324\pi$  and the laser pulse times are:  $\Gamma t_3 = 4.1470, \Gamma t_2 = 1.4122, \Gamma t_1 = 4.1470$ . The gate fidelity is  $\mathcal{F} = 0.9891$ . Another gate, the phase gate  $P = e^{-i\frac{\pi}{8}\sigma^z}$ , can likewise be simulated using the same system parameters but with the pulse times:  $\Gamma t_3 = 3.1130, \Gamma t_2 = 0.5566, \Gamma t_1 = 3.1130$ . The gate fidelity is  $\mathcal{F} = 0.9902$ . The group generated under multiplication of the set  $S = \{H, P\}$  is dense in  $SU(2)$  and  $S$  complemented by the two qubit CNOT gate is sufficient for universal quantum computation<sup>24</sup>.

Faster gate times are possible using larger field strengths and smaller detunings. For instance, for the same system parameters but with  $\kappa_3 = 200, \kappa_4 = 50$  we simulate the Hadamard with fidelity  $\mathcal{F} = 0.9709$  using the field setting  $\gamma = 0.4263\pi$  and laser pulse times:  $\Gamma t_3 = 0.2052, \Gamma t_2 = 0.4303, \Gamma t_1 = 0.2052$ . For a light hole lifetime of 50ps this corresponds to a gate time  $T_{\text{gate}} \approx 42\text{ps}$  using fields detuned by 16.7meV from optical resonance. Fidelities and gate times for generic single qubit unitaries are plotted in Fig. 6.

## V. CONCLUSIONS

We have proposed a simple way to experimentally implement arbitrary rotations with a single electron trapped in a quantum dot. As in many other works, the qubit of information is encoded in the electron spin. However, unlike in previous proposals, our procedure is based on a single laser frequency, in a one axis geometry. The latter is the laser wave vector which is set tilted with respect to the quantum dot growth direction. When the laser is detuned from the quantum dot electron-light-hole optical transition, a coherent coupling between the two spin states of the trapped electron can be induced. Moreover, in the particular experimental situation where a weak magnetic field is applied along the growth axis, setting appropriate elliptical polarizations for the addressing laser allows one to perform arbitrary single qubit rotations. These reach  $> 97\%$  fidelities, in 50ps, even in the worst scenario for which light-holes in quantum dots would exhibit a lifetime as short as in quantum wells. Furthermore, unitary operations fidelities are robust against the exact Zeeman shift of electron and hole levels, the laser detuning being in any case very large compared to these parameters. According to our analysis, in quantum dots, light-holes could become a favorable candidate for optical implementation of quantum computation protocols.

We have not addressed the issue of state preparation here. One possibility is to tune a field near resonant with the light-hole states and monitor spontaneous emission events. A null result projects the mixed qubit state into the non degenerate null space of the Hamiltonian  $\tilde{H}_m$  spanned by the computation basis states. The requirements for robust state preparation would be a decay rate fast compared to coherent dynamics in the 4 level system as well as high detector efficiency.

## Acknowledgments

F.D. appreciates many stimulating discussions with M. Combescot. F.D. and GKB received support from the Austrian Science Fund (FWF).

- 
- <sup>1</sup> S. Gulde, M. Riebe, G.P.T. Lancaster, C. Becher, J. Eschner, H. Häffner, F. Schmidt-Kaler, I.L. Chuang, and R. Blatt, *Nature* **421**, 48 (2003)
  - <sup>2</sup> F. Schmidt-Kaler, H. Häffner, M. Riebe, S. Gulde, G. P. T. Lancaster, T. Deuschle, C. Becher, C. F. Roos, J. Eschner, and R. Blatt, *Nature* **422**, 408 (2003).
  - <sup>3</sup> H. Häffner, W. Hänsel, C. F. Roos, J. Benhelm, D. Chekalkar, M. Chwalla, T. Körber, U. D. Rapol, M. Riebe, P. O. Schmidt, C. Becher, O. Gühne, W. Dür and R. Blatt, *Nature* **438**, 643 (2005).
  - <sup>4</sup> D. N. Matsukevich and A. Kuzmich, *Science* **306**, 663 (2004)
  - <sup>5</sup> D. N. Matsukevich, T. Chaneliere, S. D. Jenkins, S.-Y. Lan, T. A. B. Kennedy and A. Kuzmich, *Phys. Rev. Lett.* **96**, 30405 (2006)
  - <sup>6</sup> B. Pal, M. Ikezawa, Y. Matsumoto, I. Ignatiev, *cond-mat/0511048* (2005)
  - <sup>7</sup> M. Attature, J. Dreiser, A. Badolato, A. Högele, K. Karrai, A. Imamoglu, *Science* **312**, 551 (2006)
  - <sup>8</sup> A. S. Bracker, E. A. Stinaff, D. Gammon, M. E. Ware, J. G. Tischler, A. Shabaev, Al. L. Efros, D. Park, D. Gershoni, V. L. Korenev, and I. A. Merkulov, *Phys. Rev. Lett.* **94**, 047402 (2005)
  - <sup>9</sup> M. V. Gurudev Dutt, Jun Cheng, Bo Li, Xiaodong Xu, Xiaoqin Li, P. R. Berman, D. G. Steel, A. S. Bracker, D. Gammon, Sophia E. Economou, Ren-Bao Liu, and L. J. Sham, *Phys. Rev. Lett.* **94**, 227403 (2005)
  - <sup>10</sup> Pochung Chen, C. Piermarocchi, L. J. Sham, D. Gammon, and D. G. Steel, *Phys. Rev. B* **69**, 075320 (2004)
  - <sup>11</sup> C. Emary and L. J. Sham, *cond-mat/0608518*
  - <sup>12</sup> M. Combescot, O. Betbeder-Matibet, *Solid State Comm.* **134**, 11 (2005)
  - <sup>13</sup> Trion states in principle refer to a bound exciton interacting with an electron. However, in a quantum dot the term trion is used to describe two electrons and a hole bound by confinement.
  - <sup>14</sup> F. Troiani, E. Molinari, U. Hohenester, *Phys. Rev. Lett.* **90**, 206802 (2003)
  - <sup>15</sup> S. Sarkar, P. Palinginis, P.-C. Ku, C. J. Chang-Hasnain, N. H. Kwong, R. Binder, and H. Wang *Phys. Rev. B* **72**, 035343 (2005)
  - <sup>16</sup> T. Flissikowski, I. A. Akimov, A. Hundt, and F. Henneberger, *Phys. Rev. B* **68**, 161309(R) (2003)
  - <sup>17</sup> E. Perez, V. Bellani, S. Zimmermann, L. Munoz, L. Vina, E. S. Koteles and K. M. Lau, *Solid State Electronics* **40**, 737 (1996).
  - <sup>18</sup> T. Calarco, A. Datta, P. Fedichev, E. Pazy, P. Zoller, *Phys. Rev. A* **68** 012310 (2003)
  - <sup>19</sup> M. A. Cusack, P. R. Briddon, M. Jaros, *Phys. Rev. B* **54**, R2300 (1996)
  - <sup>20</sup> M. Combescot, *Phys. Report* **221**, 167-249 (1992)
  - <sup>21</sup> M. Combescot, *Phys. Rev. B* **41**, 3517 (1990)
  - <sup>22</sup> C. Cohen-Tannoudji, J. Dupont-Roc, G. Grynberg, *Atom-Photon Interactions, Wiley-Interscience Publication* (New-York, 1992)
  - <sup>23</sup> See e.g. J.J. Sakuri, *Modern Quantum Mechanics*, Addison-Wesley Publishing, New York (1994).
  - <sup>24</sup> P.O. Boykin, T. Mor, M. Pulver, V. Roychowdhury, F. Vatan, 40th Annu. Symp. Found. Comput. Sci. Proc. 486-494 (1999).